Published in final edited form as:
Physiol Behav. 2011 August 3; 104(2): 257–265. doi:10.1016/j.physbeh.2011.03.006.

Immune Challenge Activates Neural Inputs to the Ventrolateral Bed Nucleus of the Stria Terminalis

Michael S. Bienkowski and **Linda Rinaman**
Department of Neuroscience, University of Pittsburgh, Pittsburgh, PA

Abstract

Hypothalamo-pituitary-adrenal (HPA) axis activation in response to infection is an important mechanism by which the nervous system can suppress inflammation. HPA output is controlled by the hypothalamic paraventricular nucleus (PVN). Previously, we determined that noradrenergic inputs to the PVN contribute to, but do not entirely account for, the ability of bacterial endotoxin (i.e., lipopolysacharide, LPS) to activate the HPA axis. The present study investigated LPS-induced recruitment of neural inputs to the ventrolateral bed nucleus of the stria terminalis (vlBNST). GABAergic projections from the vlBNST inhibit PVN neurons at the apex of the HPA axis; thus, we hypothesize that LPS treatment activates inhibitory inputs to the vlBNST to thereby "disinhibit" the PVN and increase HPA output. To test this hypothesis, retrograde neural tracer was iontophoretically delivered into the vlBNST of adult male rats to retrogradely label central sources of axonal input. After one week, rats were injected i.p. with either LPS (200 μg/kg BW) or saline vehicle, and then perfused with fixative 2.5 hours later. Brains were processed for immunohistochemical localization of retrograde tracer and the immediate-early gene product, Fos (a marker of neural activation). Brain regions that provide inhibitory input to the vlBNST (e.g., caudal nucleus of the solitary tract, central amygdala, dorsolateral BNST) were preferentially activated by LPS, whereas sources of excitatory input (e.g., paraventricular thalamus, medial prefrontal cortex) were not activated or were activated less robustly. These results suggest that LPS treatment recruits central neural systems that actively suppress vlBNST neural activity, thereby removing a potent source of inhibitory control over the HPA axis.

Keywords

stress; HPA axis; inflammatory response

1. Introduction

Activation of the hypothalamo-pituitary-adrenal (HPA) axis and resulting synthesis of glucocorticoids in response to infection is an important mechanism by which the nervous system can suppress inflammation in the body. Corticotrophin-releasing hormone (CRH)-containing neurons within the paraventricular nucleus of the hypothalamus (PVN) directly stimulate the release of adrenocorticotropic hormone (ACTH) from the anterior pituitary,

Correspondence to: Dr. Linda Rinaman, Dept. Neuroscience, Univ. of Pittsburgh, 210 Langley Hall, Pittsburgh, PA 15260, rinaman@pitt.edu, 412-624-6994.

and understanding the neural network regulating CRH activation and ACTH release is crucial to understanding how the immune system interacts with the HPA axis.

In response to systemic infection, peripheral immune cells signal the brain by releasing various pro-inflammatory cytokines. Cytokines can access the nervous system directly by entering central perivascular spaces via diffusion at circumventricular organs (CVOs) that lack a blood-brain barrier, or indirectly by stimulating paracrine release of prostaglandins from medullary perivascular cells and via peripheral activation of receptor-mediated mechanisms involving vagal sensory afferents [1–5]. Both direct and indirect mechanisms of cytokine action converge at the nucleus of the solitary tract (NTS), a hindbrain region that is strategically located to detect immune signals via its connections with the area postrema, a CVO [6], and through direct inputs from vagal sensory afferents [7]. In a previous study, we determined that noradrenergic (NA) neurons within the NTS and ventrolateral medulla (VLM) are essential modulators of excitatory neurotransmission to the PVN in rats after systemic administration of lipopolysaccharide (LPS) [8], a major component of the protein coat of gram-negative bacteria. Interestingly, lesioning NA inputs to the PVN attenuated but did not abolish PVN neural Fos expression or plasma corticosterone responses to LPS treatment [8], evidence that additional brain regions and/or neurochemical signaling pathways contribute to HPA axis activation after immune challenge.

A potential candidate region for mediating non-NA influences on the PVN after immune challenge is the bed nucleus of the stria terminalis (BNST), located within the basal forebrain. Portions of the BNST directly innervate the PVN [9], and the BNST is anatomically positioned to serve as a relay for mediating the influence of several forebrain brain regions on HPA function, including the central nucleus of the amygdala (CEA), ventral subiculum, and medial prefrontal cortex (mPFC) [10–14]. Previous studies examining the functional anatomy of LPS- or interleukin-1β (IL1β)-induced neural Fos expression have identified the dorsolateral BNST (dlBNST) as a particularly sensitive region that is highly activated by immune challenge, perhaps due to its inputs from activated neurons within the NTS, VLM, and parabrachial nucleus (PBN) [7, 15–18]. Thus, the dlBNST is a strong candidate for mediating immune influences on the HPA axis. However, very few dlBNST neurons project to the PVN. Instead, PVN inputs from the BNST derive primarily from its ventrolateral subnuclei (vlBNST), which contain relatively few Fos-positive neurons after LPS treatment [8, 19, 20]. Although discrete lesions of the dlBNST do not alter the ability of systemic cytokine administration to activate CRH-positive PVN neurons, PVN Fos activation is attenuated after larger lesions that also include the vlBNST [19]. The available evidence suggests that BNST-derived regulation of HPA responses to immune challenge is accomplished through di- or multisynaptic circuits involving the BNST and/or CEA [21]. In support of this, our previous study revealed a trend towards *reduced* vlBNST Fos expression in LPS-treated rats compared to saline-treated controls, whereas LPS treatment markedly increased Fos expression within the dlBNST [8].

The present study was designed to identify potential central sources of inhibitory input to the vlBNST that are Fos-activated in rats after LPS treatment. In particular, we examined the possibility that LPS-activated neurons within the dlBNST and CEA project to the vlBNST. Since neurons within the dlBNST, CEA, and vlBNST are primarily GABAergic, LPS-induced activation of dlBNST or CEA neurons that innervate the vlBNST would promote inhibition of vlBNST inputs to the PVN, thereby disinhibiting CRH neurons at the apex of the HPA axis. Iontophoretic delivery of the retrograde tracer Fluorogold (FG) or cholera toxin subunit beta (CTb) was targeted specifically to the vlBNST of adult male rats, and retrogradely-labeled neurons within the dlBNST, CEA and other brain regions (i.e., NTS, VLM, PBN, paraventricular thalamus (PVT), and mPFC) were examined for LPS-induced Fos expression. Our results support the view that immune challenge activates several brain

regions with axonal inputs to the vlBNST that likely contribute to suppression of vlBNST neural activity, thereby suppressing its inhibitory influence on CRH neurons within the PVN.

2. Methods

2.1 Animals

Adult male Sprague-Dawley rats (200–300g BW; Harlan Laboratories, Indianapolis, IN, USA) were individually housed in stainless steel hanging cages in a controlled environment (20–22°C, 12:12 hr light:dark cycle; lights off at 1900 hr) with *ad libitum* access to water and pelleted chow (Purina 5001). Experimental protocols were approved by the University of Pittsburgh Institutional Animal Care and Use Committee, and were carried out in accordance with the National Institutes of Health Guide for the Care and Use of Laboratory Animals, with efforts to minimize both the number of animals used and their potential discomfort.

2.2 Iontophoretic Tracer Delivery

Rats were anesthetized by halothane or isoflurane inhalation (Halocarbon Laboratories, River Edge, NJ; 1–3% in oxygen) and oriented into a Kopf stereotax in the flat skull position. Using a dental drill, a small hole (~1–2 mm diameter) was opened in the skull to expose the cortical surface overlying the vlBNST tracer delivery target site. A pulled glass micropipette (approximately 20 μm outer tip diameter) was attached to the arm of the stereotax. Using negative pressure, the micropipette was backfilled with a 1–2% solution of Fluorogold (FG; Fluorochrome) diluted in 0.1M cacodylic acid or with 1% CTb diluted in 0.1M phosphate buffer (pH=6.0), and then a microwire connected to a current source (Stoelting) was lowered into the tracer solution. A 0.5 μA retaining current was applied to minimize molecular diffusion of tracer from the pipette tip as it was lowered into the brain. FG or CTb was unilaterally iontophoresed into the vlBNST (bregma: −0.3 posterior, +2.8 lateral, −7.0 ventral; 10° angle) using a 7 s pulsed positive current of 5 μA for a duration of 5 min. Iontophoretic parameters were determined through pilot studies and were found to produce discrete, localized tracer delivery sites with minimal tracer diffusion into regions adjacent to the vlBNST. The micropipette tip was left in place for 5 min after iontophoresis, and then was withdrawn. The skin over the skull was closed with stainless steel clips and rats were injected with 1 mg of analgesic (Ketofen; 0.5 ml, s.c.). Rats were returned to their home cage after regaining consciousness and full mobility.

After a 7–14 d post-iontophoresis survival time, animals were injected i.p. with 2.0 ml of 0.15M NaCl containing LPS at a dose of 200 μg/kg BW (n=8), or were injected with the same volume of vehicle alone (n=6). After injection, rats were returned to their home cage and left undisturbed for 2.5–3 h, then deeply anesthetized with sodium pentobarbital (Nembutal, 100 mg/kg BW, i.p.) and transcardially perfused with 100 ml saline followed by 500 ml of fixative (4% paraformaldehyde in 0.1M phosphate buffer). This LPS dose and post-injection survival time were selected to match those used in our previous study [8] in order to maximize the number of Fos-positive neurons visualized after LPS challenge [16, 18]. Brains were postfixed *in situ* overnight at 4°C then removed from the skull and cryoprotected in 20% sucrose solution for 24–72 hr. Brains were sectioned coronally (35 μm) using a freezing microtome. Sections were collected sequentially into 6 adjacent sets and were stored in cryopreservant [22] at −20°C for later immunohistochemical processing.

2.3 Immunohistochemistry

One tissue section series (containing sections spaced by 210 μm) from each rat was used for dual immunoperoxidase localization of nuclear Fos protein and cytoplasmic neural tracer

(either FG or CTb). Tissue sections were removed from storage and rinsed in buffer (0.1M sodium phosphate, pH=7.4) for 1 h prior to immunohistochemical procedures. Immunoperoxidase localization of Fos protein followed previously established protocols [8, 23]. Tissue sections were incubated overnight in sodium phosphate buffer containing 0.3% Triton-X100, 1% normal donkey serum, 1% bovine serum albumin (BSA), and a rabbit polyclonal anti-Fos antibody (1:50,000, Dr. Philip Larsen, Denmark). The specificity of this antibody for Fos protein has been established [23]. After buffer rinsing, sections were incubated in biotinylated donkey anti-rabbit IgG (1:500; Jackson Immunochemicals) and Vectastatin ABC Elite reagents (Vector Laboratories, Burlingame, CA, USA) followed by a solution of nickel sulfate and diaminobenzidine (DAB) with hydrogen peroxidase to produce a blue-black reaction product within the nucleus of Fos-positive neurons. Sections then were rinsed in buffer and incubated overnight in primary antiserum to localize neural tracer [either goat anti-CTb (1:50,000; List Biological Laboratories) or rabbit anti-FG (1:30,000; Chemicon International) diluted in buffer containing 0.3% Triton X100 and 1% normal donkey serum. After rinsing, sections were incubated in biotinylated secondary donkey anti-goat or anti-rabbit IgG (1:500) and Vectastatin ABC Elite reagents followed by a non-intensified DAB-hydrogen peroxidase reaction to produce brown immunoprecipitate localizing the neural tracer delivery site and retrogradely-labeled neurons. Immunostained tissue sections were rinsed in buffer, mounted onto Superfrost Plus microscope slides (Fisher Scientific), allowed to dry overnight, dehydrated and defatted in graded ethanols and xylene, and coverslipped using Cytoseal 60 (VWR).

2.4 Quantification of tracer- and Fos-positive neurons

Dual-immunoperoxidase labeled tissue sections from each rat were analyzed using a light microscope to determine the number and proportion of retrogradely–labeled BNST afferents activated to express Fos after LPS or control saline treatment. Criteria for counting tracer-positive neurons included the presence of brown cytoplasmic immunoreactivity and a visible nucleus. Tracer-positive neurons in which the nucleus contained blue-black Fos immunoreactivity were considered double-labeled, regardless of Fos labeling intensity. Using a 40x microscope objective, tracer-positive neurons were quantified bilaterally in sections spaced by 210 μm through the NTS, VLM, lateral PBN, PVT, medial and lateral CEA (mCEA, lCEA), and dlBNST. As noted in the results, exceedingly few of the retrogradely-labeled neurons within the mPFC expressed Fos in rats after either LPS or saline treatment (i.e., fewer than 3–5 neurons per rat, regardless of treatment), and so mPFC labeling was not quantified. Counts of retrogradely-labeled NTS and VLM neurons were initiated caudal to obex (i.e., ~630 μm caudal to the area postrema (AP) and ~14.6 mm caudal to bregma], and concluded just rostral to the AP (i.e., ~13.2 mm caudal to bregma), comprising 7–8 tissue sections (spaced by 210 μm) per rat. Retrogradely-labeled neurons in the lateral PBN, mCEA, lCEA, and dlBNST were counted bilaterally in sections identified as containing the highest incidence of Fos-positive neurons in LPS-treated rats. This included 4 sections through the PBN (~9.3 mm-8.2 mm caudal to bregma), 3 sections through the mCEA and lCEA (~3.3-2.8 mm caudal to bregma), and 3 sections through the dlBNST (~0.3 mm caudal to bregma through 0.2 mm rostral to bregma). Counts of retrogradely-labeled PVT neurons were made throughout the rostrocaudal extent of the PVT (approximately 13 sections, ~4.16-0.92 mm caudal to bregma).

2.5 Data analysis

For statistical comparisons of labeling patterns within and between groups, ipsilateral and contralateral cell counts of each brain region were combined to obtain the total number of single-labeled (tracer only) and double-labeled (tracer+Fos) neurons for each region. Counts made within the NTS, VLM, and PVT also were analyzed by rostrocaudal level through each region. The percentage of activated neurons within each region was calculated as

(tracer+Fos)/[(tracer only)+(tracer+Fos)]×100. For each brain region, a one-way ANOVA was conducted on total cell counts to examine the effect of LPS vs. saline control treatment on the number of tracer-labeled neurons (with no effect expected), and on Fos activation of tracer-labeled neurons. For the NTS, VLM, and PVT, the potential effect of rostrocaudal level on retrograde labeling and/or Fos activation also was analyzed using repeated-measures ANOVA, with rostrocaudal level as the repeated measure. Differences and interaction effects were considered significant when $P < 0.05$.

3. Results

3.1 Iontophoretic delivery of retrograde tracer into the vlBNST

FG or CTb was accurately iontophoresed into the vlBNST in 14 animals, with minimal or no tracer delivery into the adjacent posterior BNST, dlBNST, ventral pallidum, or lateral preoptic area. The relative lack of tracer delivery into adjacent regions in rats with "accurate" placements was confirmed by comparing retrograde labeling in accurate cases with the different patterns of retrograde labeling produced in rats in which tracer was inadvertently delivered into one or more of these adjacent regions (data not shown). Accurate iontophoresis produced spherical tracer delivery sites that were centered in the region containing the anterolateral and fusiform subnuclei of the vlBNST (Fig. 1). Tracer delivery sites and the quality of retrograde labeling were similar in rats iontophoresed with either FG or CTb. Further, there were no significant tracer-related differences in the number of retrogradely-labeled neurons in any brain region subjected to quantitative analysis. Thus, data generated with either tracer were combined and are presented together.

3.2 Distribution of retrogradely-labeled neurons

3.2.1 Medulla—Tracer deposits in the vlBNST produced a pattern of retrograde labeling consistent with previous reports [12, 24]. Within the medulla, retrogradely-labeled neurons were located primarily within the caudal (i.e., visceral) NTS and caudal VLM. Tracer-labeled NTS neurons were concentrated ipsilateral to the tracer delivery site, and were distributed from the most caudal levels of the NTS (~14.6 mm caudal to bregma) through anterior levels just rostral to the AP, where the NTS separates from the floor of the fourth ventricle (~13.2 mm caudal to bregma). Quantification of labeling in a 1:6 series of sections revealed a total average of 156±10 retrogradely-labeled NTS neurons per case, with peak labeling at the rostrocaudal level of the AP (Fig. 2A,B; Fig. 3A). Retrogradely-labeled VLM neurons were distributed at similar rostrocaudal levels as NTS labeling, although VLM labeling was more bilaterally distributed and was characterized by a relatively consistent number of labeled neurons across rostrocaudal levels (total average 80±7 neurons per case) (Fig. 2C,D; Fig. 3B). Statistical analysis revealed that the NTS contained a significantly greater number of retrogradely-labeled neurons compared to the VLM ($p<0.0005$).

3.2.2 Pons—Retrogradely-labeled neurons within the pons were concentrated in the parabrachial nucleus (PBN), with smaller numbers of neurons scattered within the locus coeruleus and the pre-locus coeruleus region primarily ipsilateral to the vlBNST tracer delivery site. Within the ipsilateral PBN, retrogradely-labeled neurons were located mainly in the medial and central lateral subnuclei at caudal levels (i.e., ~ 9.7 mm caudal to bregma), with relatively few tracer-labeled neurons present within the same PBN subnuclei contralateral to the vlBNST tracer delivery site. However, retrograde labeling within the PBN was more prevalent at more rostral levels (i.e., ~ 8.7 mm caudal to bregma), where labeling was concentrated in the lateral PBN (Fig. 3C). Quantitative analysis of lateral PBN labeling revealed a total average of 79±10 retrogradely-labeled neurons ipsilateral to the tracer delivery site, and a total average of 21±3 retrogradely-labeled neurons contralaterally.

3.2.3 Forebrain—Retrogradely-labeled neurons were present within multiple regions of the hypothalamus, thalamus, basal forebrain, and cortex, including several areas associated with coordinating stress responses (i.e., PVT, CEA, mPFC, dlBNST). Retrogradely-labeled neurons were present throughout the rostrocaudal extent of the PVT ipsilateral to the tracer delivery site (Fig. 2E,F; Fig. 4A,B). Quantification supported previous qualitative observations [24] that the number of vlBNST-projecting neurons in the rostral half of the PVT (rPVT, 314±23) was significantly greater than in the caudal half of the PVT (cPVT, 175±12; $p<0.0005$; Fig. 2E,F).

Within the amygdala, dense retrograde labeling was observed in the ipsilateral posterior basolateral amygdala, basomedial amygdala, and CEA, with only sparse contralateral labeling. Quantitative analysis revealed a significantly greater number of retrogradely-labeled neurons within the mCEA (256±27) compared to the lCEA (168±23; $p<0.05$) (Fig. 4C).

Retrograde labeling within the dlBNST also displayed a strong ipsilateral predominance. Labeled neurons were distributed throughout the oval, juxtacapsular, and anterolateral subnuclei of the dlBNST (totaling an average of 540±20 neurons per case), and were most dense just rostral to the midline crossing of the anterior commissure (~0.2 mm caudal to bregma) (Fig. 1; Fig. 4D). Retrograde labeling within the mPFC was present in both prelimbic and infralimbic regions.

3.3 Treatment-induced activation of retrogradely-labeled neurons

Animals in this study were not handled or acclimated to i.p. injections before treatment with saline or LPS. Accordingly, Fos labeling in saline-injected control rats reflects baseline neural activation plus additional activation associated with the mild stress of handling and i.p. injection. In these control animals, Fos expression within the NTS, lateral PBN, CEA, and dlBNST was relatively low compared to Fos expression in LPS-treated rats (Fig. 2A,B, Fig. 5), whereas more comparable levels of Fos expression were observed within the VLM (Fig. 2C,D; Fig. 5) and throughout the rostrocaudal extent of the PVT (Fig. 2E,F; Fig. 5) regardless of i.p. treatment group. Extremely few retrogradely-labeled neurons within the mPFC expressed Fos in either LPS-treated or control rats (i.e., less than 4–5 neurons per rat, regardless of treatment: data not shown). The overall pattern of LPS-induced Fos expression was consistent with previous reports [25].

Quantification confirmed that the proportion of the total populations of retrogradely-labeled neurons within the NTS, VLM, lateral PBN, and dlBNST that were activated to express Fos was significantly greater in LPS-treated rats compared to saline controls (Fig. 5; $P < 0.005$ for each region; Table 1). Conversely, despite the preponderance of retrograde labeling within the mCEA vs. the lCEA, only the lCEA contained significant higher proportions of tracer-labeled neurons expressing Fos in LPS-treated rats vs. saline controls (Fig. 5; Table 1). Despite widespread Fos expression within the mPFC, very few retrogradely-labeled mPFC neurons were Fos-positive in LPS or saline-injected animals, consistent with a previous report examining Fos expression in rats after systemic administration of the cytokine IL1β [12].

4. Discussion

Results from the present study reveal several key brainstem and forebrain regions that innervate the vlBNST and are activated in rats after LPS-induced immune challenge. These regions include the NTS, VLM, lateral PBN, lateral CEA, and the dlBNST. As discussed further, below, several of these regions are known to exert an inhibitory influence over vlBNST neural activity. Conversely, LPS treatment did not significantly activate vlBNST-

projecting neurons within the mCEA, cPVT, or mPFC compared to activation after control saline treatment. Considered together with previous findings, these results suggest that vlBNST neuronal activity is actively suppressed by at least a subset of its afferent inputs during the acute phase of the inflammatory response. Since vlBNST projections to the medial parvocellular PVN are primarily (or exclusively) inhibitory, active suppression of vlBNST activity would promote disinhibition of CRH neurons at the apex of the HPA axis, thereby increasing plasma ACTH and corticosterone responses during acute immune challenge.

4.1 vlBNST inputs from the NTS and VL

After delivery of retrograde tracer into the vlBNST, the caudal NTS and VLM contained large numbers of retrogradely-labeled neurons, and a significantly greater proportion of these neurons expressed Fos in rats after LPS vs. control saline treatment. The caudal NTS and VLM contain the A2 and A1 noradrenergic (NA) cell groups, respectively, which provide the vlBNST with the densest NA terminal field present within the brain [26]. The majority of NTS and VLM neurons that innervate the vlBNST are NA neurons [24, 27], and LPS treatment activates the large majority of NA neurons within the NTS and VLM [8, 18]. Electrophysiological experiments have demonstrated that norepinephrine injected into the vlBNST suppresses local glutamatergic transmission via the α_{2A}-adrenergic receptor, and increases local GABAergic transmission via α_1-adrenergic receptors [28–31]. The receptor-mediated effects of norepinephrine in the vlBNST promote inhibition of vlBNST neuron firing, which consequently suppresses GABAergic signaling from the vlBNST to the PVN [32]. Thus, LPS-induced recruitment of NA inputs from the NTS and VLM is consistent with an active inhibition of vlBNST neuronal activity during the inflammatory immune response.

4.2 vlBNST inputs from the lateral PBN

Results from a study in which the lateral PBN was lesioned indicate that this pontine region contributes importantly to the ability of acute immune challenge to increase Fos expression within the CEA and dlBNST [17]. Results from the present study reveal that lateral PBN neurons projecting directly to the vlBNST also are activated in rats after LPS treatment, although the role of this input in modulating vlBNST activity is unknown. Lateral PBN neurons express several different peptidergic neurotransmitters, including calcitonin gene-related peptide, substance P, neurotensin, somatostatin, enkephalin, and cholecystokinin [33–35]. Further study is needed to determine the physiological role of PBN axonal inputs to the vlBNST.

4.3 vlBNST inputs from the PVT

The PVT is implicated in relaying interoceptive (i.e., visceral) sensory signals to the forebrain, including signals generated during stressful challenges [36–38]. The caudal PVT appears to be involved in the ability of chronic stress to facilitate HPA axis responses to an acute novel stressor, while the rostral PVT receives dense inputs from the hypothalamic suprachiasmatic nucleus (SCN) that may modulate stress responses across the circadian cycle [39]. Our results confirmed previous qualitative reports that the vlBNST is innervated more prevalently by the rPVT compared to the cPVT [24]. Quantification of retrogradely-labeled neurons across the rostrocaudal extent of the PVT in this study revealed that acute LPS administration produced a small yet significant increase in activated vlBNST-projecting neurons in the rPVT, but not in the cPVT, as compared to activation in saline-injected control rats. This study adds to the growing evidence that rostral and caudal areas of the PVT differentially regulate certain aspects of the stress response.

PVT projection neurons are glutamatergic [40], suggesting that LPS-activated inputs from the rPVT would promote excitation of vlBNST target neurons. Additional work is needed to identify the relative functional significance and postsynaptic targets of this glutamatergic input to the vlBNST, and to evaluate whether this input complements or antagonizes what appears to otherwise be predominantly inhibitory inputs to the vlBNST that are recruited during the immune response.

4.4 vlBNST inputs from the forebrain

Large numbers of neurons within the CEA, dlBNST, and mPFC were retrogradely labeled following tracer delivery into the vlBNST. Although larger numbers of vlBNST afferent neurons were located within the mCEA compared to the lCEA, LPS treatment differentially activated only the lCEA population. Interestingly, a similar finding has been reported for lCEA vs. mCEA neurons innervating the BNST in rats after treatment with the cytokine IL-1β [19], although that study did not determine whether the CEA neurons were targeting the dlBNST, vlBNST, or both. Projection neurons within the dlBNST and CEA are primarily (if not exclusively) GABAergic, consistent with the proposal that LPS-induced activation of vlBNST-projecting neurons within the lCEA and dlBNST promotes inhibition of target neurons within the vlBNST.

Previous reports indicated that lesions of the ventral mPFC can enhance HPA axis responses to immune challenge (i.e., systemic administration of IL1β), although mPFC neurons that project directly to the vlBNST were not activated by this treatment [12]. Our qualitative observations of retrograde labeling and LPS-induced Fos expression within the mPFC are consistent with that earlier report. Although many retrogradely-labeled neurons were present within the mPFC, exceedingly few were double-labeled for Fos in rats after either LPS or saline control treatment, evidence that glutamatergic cortical inputs to the vlBNST are not recruited during the acute LPS-induced inflammatory response.

4.5 Summary and conclusions

Previous retrograde tracing studies examining LPS or cytokine-stimulated recruitment of neural inputs to the BNST either examined inputs to the dlBNST [41], or focused exclusively on inputs arising from the mPFC [12]. The present report is the first to examine LPS-induced recruitment of multiple sources of central input to the vlBNST, an important constituent of the brain's immune response network. The schematic in Figure 6 summarizes our main results. The pattern of Fos-activated neural inputs to the vlBNST supports the view that these inputs collectively promote an active inhibition of vlBNST activity during the acute inflammatory response to LPS. NA inputs from the caudal NTS and VLM are known to modulate local glutamatergic and GABAergic signaling to promote inhibition of vlBNST activity. Additional GABAergic inputs to the vlBNST arising from the lCEA and dlBNST also are highly activated during the inflammatory response, while glutamatergic inputs from the mPFC are not activated and those from the rPVT are relatively minimal. The hypothesized resulting suppression of neural activity within the vlBNST removes a source of inhibitory input to CRH-positive PVN neurons at the apex of the HPA axis, as well as to the other projection targets of GABAergic vlBNST neurons [42].

Acknowledgments

Research supported by NIH grant MH59911 to L.R.

References Cited

1. Buller KM. Circumventricular organs: gateways to the brain role of circumventricular organs in pro-inflammatory cytokine-induced activation of the hypothalamic- pituitary-adrenal axis. Clinical and Experimental Pharmacology and Physiology. 2001; 28:581–589. [PubMed: 11458886]
2. Ek M, Kurosawa M, Lundeberg T, Ericsson A. Activation of vagal afferents after intravenous injection of interleukin-1beta : role of endogenous prostaglandins. J. Neurosci. 1998; 18:9471–9479. [PubMed: 9801384]
3. Vitkovic L, Konsman JP, Bockaert J, Dantzer R, Homburger V, Jacque C. Cytokine signals propagate through the brain. Molecular Psychiatry. 2000; 5:604–615. [PubMed: 11126391]
4. Ericsson A, Arias C, Sawchenko PE. Evidence for an intramedullary prostaglandin-dependent mechanism in the activation of stress-related neuroendocrine circuitry by intravenous interleukin-1. J. Neurosci. 1997; 17:7166–7179. [PubMed: 9278551]
5. Goehler, LE.; Gaykema, RPA. Neural pathways mediating behavioral changes associated with immunological challenge. In: Siegal, A.; Zalcman, S., editors. The Neuroimmunological Basis of Behavior and Mental Disorders. 1st ed.. New York: Springer; 2008.
6. Lee HY, Whiteside MB, Herkenham M. Area postrema removal abolishes stimulatory effects of intravenous interleukin-1[beta] on hypothalamic-pituitary-adrenal axis activity and c-fos mRNA in the hypothalamic paraventricular nucleus. Brain Research Bulletin. 1998; 46:495–503. [PubMed: 9744286]
7. Ericsson A, Kovacs KJ, Sawchenko PE. A functional anatomical analysis of central pathways subserving the effects of interleukin-1 on stress-related neuroendocrine neurons. J. Neurosci. 1994; 14:897–913. [PubMed: 8301368]
8. Bienkowski MS, Rinaman L. Noradrenergic inputs to the paraventricular hypothalamus contribute to hypothalamic-pituitary-adrenal axis and central Fos activation in rats after acute systemic endotoxin exposure. Neuroscience. 2008; 156:1093–1102. [PubMed: 18773942]
9. Elmquist JK, Saper CB. Activation of neurons projecting to the paraventricular hypothalamic nucleus by intravenous lipopolysaccharide. The Journal of Comparative Neurology. 1996; 374:315–331. [PubMed: 8906501]
10. Cullinan WE, Herman JP, Watson SJ. Ventral subicular interaction with the hypothalamic paraventricular nucleus: evidence for a relay in the bed nucleus of the stria terminalis. The Journal of Comparative Neurology. 1993; 332:1–20. [PubMed: 7685778]
11. Ziegler DR, Herman JP. Neurocircuitry of stress integration: anatomical pathways regulating the hypothalamo-pituitary-adrenocortical axis of the rat. Integr. Comp. Biol. 2002; 42:541–551.
12. Crane JW, Ebner K, Day TA. Medial prefrontal cortex suppression of the hypothalamic–pituitary–adrenal axis response to a physical stressor, systemic delivery of interleukin-1β. Blackwell Science, Ltd. 2003:1473–1481.
13. Radley JJ, Gosselink KL, Sawchenko PE. A discrete GABAergic relay mediates medial prefrontal cortical inhibition of the neuroendocrine stress response. J. Neurosci. 2009; 29:7330–7340. [PubMed: 19494154]
14. Buller KM, Crane JW, Day TA. The central nucleus of the amygdala; a conduit for modulation of HPA axis responses to an immune challenge? Stress: The International Journal on the Biology of Stress. 2001; 4:277–287.
15. Vallières L, Lacroix S, Rivest S. Influence of interleukin-6 on neural activity and transcription of the gene encoding corticotrophin-releasing factor in the rat brain: an effect depending upon the route of administration. European Journal of Neuroscience. 1997; 9:1461–1472. [PubMed: 9240403]
16. Hare AS, Clarke G, Tolchard S. Bacterial lipopolysaccharide-induced changes in Fos protein expression in the rat brain: correlation with thermoregulatory changes and plasma corticosterone. Journal of Neuroendocrinology. 1995; 7:791–799. [PubMed: 8563722]
17. Buller KM, Allen T, Wilson LD, Munro F, Day TA. A critical role for the parabrachial nucleus in generating central nervous system responses elicited by a systemic immune challenge. Journal of Neuroimmunology. 2004; 152:20–32. [PubMed: 15223234]

18. Marvel FA, Chen C-C, Badr N, Gaykema RPA, Goehler LE. Reversible inactivation of the dorsal vagal complex blocks lipopolysaccharide-induced social withdrawal and c-Fos expression in central autonomic nuclei. Brain, Behavior, and Immunity. 2004; 18:123–134.
19. Crane JW, Buller KM, Day TA. Evidence that the bed nucleus of the stria terminalis contributes to the modulation of hypophysiotropic corticotropin-releasing factor cell responses to systemic interleukin-1beta. The Journal of Comparative Neurology. 2003; 467:232–242. [PubMed: 14595770]
20. Day H, Curran E, Watson S, Akil H. Distinct neurochemical populations in the rat central nucleus of the amygdala and bed nucleus of the stria terminalis: evidence for their selective activation by interleukin-1B. Journal of Comparative Neurology. 1999; 413:113–128. [PubMed: 10464374]
21. Choi DC, Furay AR, Evanson NK, Ostrander MM, Ulrich-Lai YM, Herman JP. Bed nucleus of the stria terminalis subregions differentially regulate hypothalamic-pituitary-adrenal axis activity: implications for the integration of limbic inputs. J. Neurosci. 2007; 27:2025–2034. [PubMed: 17314298]
22. Watson RE, Wiegand SJ, Clough RW, Hoffman GE. Use of cryoprotectant to maintain long-term peptide immunoreactivity and tissue morphology. Peptides. 1986; 7:155–159. [PubMed: 3520509]
23. Rinaman L, Stricker EM, Hoffman GE, Verbalis JG. Central c-Fos expression in neonatal and adult rats after subcutaneous injection of hypertonic saline. Neuroscience. 1997; 79:1165–1175. [PubMed: 9219975]
24. Shin J-W, Geerling JC, Loewy AD. Inputs to the ventrolateral bed nucleus of the stria terminalis. The Journal of Comparative Neurology. 2008; 511:628–657. [PubMed: 18853414]
25. Sagar SM, Price KJ, Kasting NW, Sharp FR. Anatomic patterns of FOS immunostaining in rat brain following systemic endotoxin administration. Brain Research Bulletin. 1995; 36:381–392. [PubMed: 7712198]
26. Brownstein, MJ.; Palkovits, M. Classical neurotransmitters in the CNS, Part 1. In: Bjorklund, A.; Hokfelt, T., editors. Handbook of Chemical Neuroanatomy. Amsterdam: Elselvier; 1984. p. 23-54.
27. Delfs JM, Zhu Y, Druhan JP, Aston-Jones G. Noradrenaline in the ventral forebrain is critical for opiate withdrawal-induced aversion. Nature. 2000; 403:430–434. [PubMed: 10667795]
28. Casada JH, Dafny N. Responses of neurons in bed nucleus of the stria terminalis to microiontophoretically applied morphine, norepinephrine and acetylcholine. Neuropharmacology. 1993; 32:279–284. [PubMed: 8474624]
29. Egli RE, Kash TL, Choo K, Savchenko V, Matthews RT, Blakely RD, et al. Norepinephrine modulates glutamatergic transmission in the bed nucleus of the stria terminalis. Neuropsychopharmacology. 2004; 30:657–668. [PubMed: 15602500]
30. McElligott ZA, Winder DG. Modulation of glutamatergic synaptic transmission in the bed nucleus of the stria terminalis. Progress in Neuro-Psychopharmacology and Biological Psychiatry. 2009; 33:1329–1335. [PubMed: 19524008]
31. Dumont EC, Williams JT. Noradrenaline triggers GABAA inhibition of bed nucleus of the stria terminalis neurons projecting to the ventral tegmental area. J. Neurosci. 2004; 24:8198–8204. [PubMed: 15385602]
32. Forray MI, Gysling K. Role of noradrenergic projections to the bed nucleus of the stria terminalis in the regulation of the hypothalamic-pituitary-adrenal axis. Brain Research Reviews. 2004; 47:145–160. [PubMed: 15572169]
33. Block CH, Hoffman GE. Neuropeptide and monoamine components of the parabrachial pontine complex. Peptides. 1987; 8:267–283. [PubMed: 2884646]
34. Block CH, Hoffman G, Kapp BS. Peptide-containing pathways from the parabrachial complex to the central nucleus of the amygdala. Peptides. 1989; 10:465–471. [PubMed: 2474157]
35. Schwaber JS, Sternini C, Brecha NC, Rogers WT, Card JP. Neurons containing calcitonin gene-related peptide in the parabrachial nucleus project to the central nucleus of the amygdala. Alan R. Liss, Inc. 1988:416–426.
36. Spencer SJ, Fox JC, Day TA. Thalamic paraventricular nucleus lesions facilitate central amygdala neuronal responses to acute psychological stress. Brain Research. 2004; 997:234–237. [PubMed: 14706875]

37. Fernandes GA, Perks P, Cox NKM, Lightman SL, Ingram CD, Shanks N. Habituation and cross-sensitization of stress-induced hypothalamic-pituitary-adrenal activity: effect of lesions in the paraventricular nucleus of the thalamus or bed nuclei of the stria terminalis. Blackwell Science, Ltd. 2002:593–602.

38. Herman JP, Figueiredo H, Mueller NK, Ulrich-Lai Y, Ostrander MM, Choi DC, et al. Central mechanisms of stress integration: hierarchical circuitry controlling hypothalamo-pituitary-adrenocortical responsiveness. Frontiers in Neuroendocrinology. 2003; 24:151–180. [PubMed: 14596810]

39. Bhatnagar S, Dallman M. Neuroanatomical basis for facilitation of hypothalamic-pituitary-adrenal responses to a novel stressor after chronic stress. Neuroscience. 1998; 84:1025–1039. [PubMed: 9578393]

40. Huang H, Ghosh P, van den Pol AN. Prefrontal cortex-projecting glutamatergic thalamic paraventricular nucleus-excited by hypocretin: a feedforward circuit that may enhance cognitive arousal. J Neurophysiol. 2006; 95:1656–1668. [PubMed: 16492946]

41. Gaykema RPA, Chen C-C, Goehler LE. Organization of immune-responsive medullary projections to the bed nucleus of the stria terminalis, central amygdala, and paraventricular nucleus of the hypothalamus: Evidence for parallel viscerosensory pathways in the rat brain. Brain Research. 2007; 1130:130–145. [PubMed: 17169348]

42. Dong H-W, Petrovich GD, Watts AG, Swanson LW. Basic organization of projections from the oval and fusiform nuclei of the bed nuclei of the stria terminalis in adult rat brain. The Journal of Comparative Neurology. 2001; 436:430–455. [PubMed: 11447588]

43. Swanson, LW. Brain maps: structure of the rat brain. Third Edition. San Diego, CA: Elselvier; 2004.

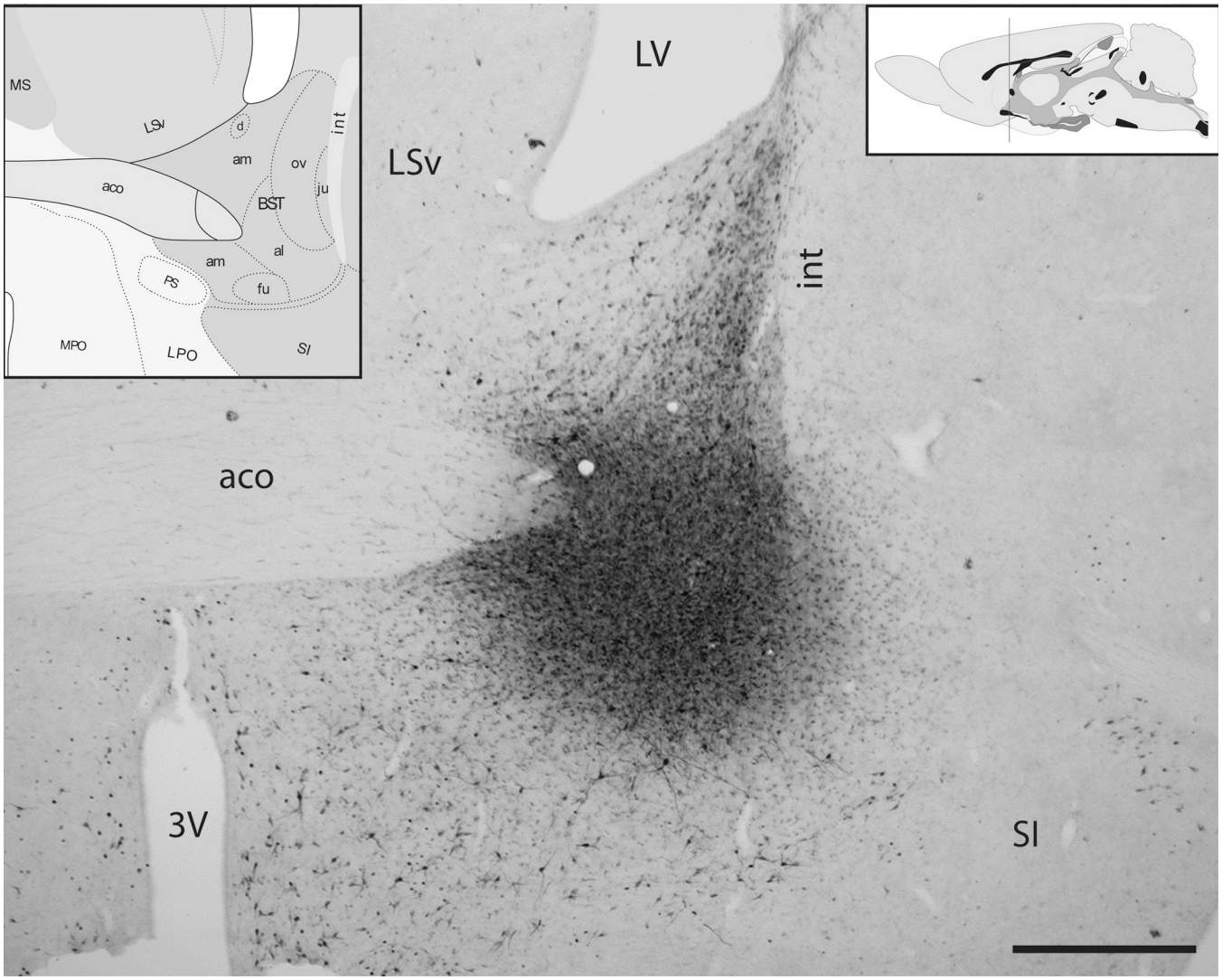

Figure 1. Retrograde tracer delivery site in the vlBNST

Iontophoretic delivery of FG (shown here) or CTb produced spherical tracer delivery sites. Iontophoretic sites were considered accurate if they were centered within the anterolateral (al) and fusiform (fu) subnuclei of the vlBNST, with minimal spread of the surrounding halo into adjacent regions. Note that labeling observed within the oval subnucleus of the dorsal BNST (ov) and other nearby regions is the product of retrograde transport from the vlBNST tracer delivery site. Atlas figures (insets) from Swanson [43]. The vertical line in the upper right inset indicates the approximate rostrocaudal level depicted in the photomicrograph. *3V=third ventricle, aco= anterior commissure, int=internal capsule, LSv=ventral lateral septum, LV= lateral ventricle, SI=substantia innominata*. Scale bar= 1 mm.

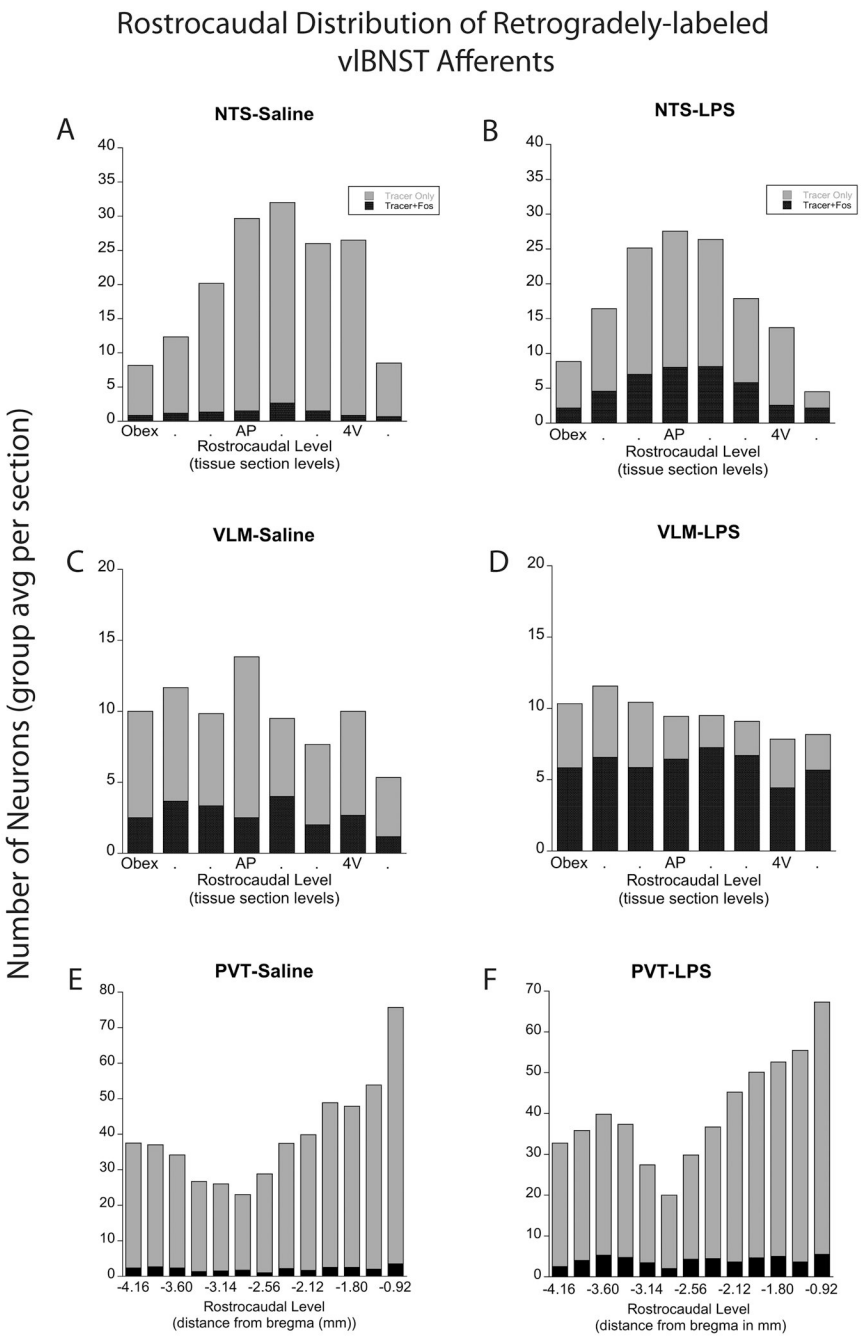

Figure 2. Rostrocaudal distribution of retrogradely-labeled neurons in the NTS, VLM, and PVT

Rostrocaudal distribution of retrograde labeling in the NTS, VLM, and PVT in rats after control saline (left panels; n=6) or LPS treatment (right panels; n=8). The number of single- and double-labeled NTS neurons (A, B) was greatest at the rostrocaudal level of the mid area postrema (AP) and just rostral to it. Within the VLM (C, D), single- and double-labeled neurons were distributed more evenly across rostrocaudal levels. The proportion of tracer-labeled NTS and VLM neurons that expressed Fos was significantly increased in rats after LPS treatment (see Fig. 5 and Table 1). Larger numbers of tracer-labeled neurons were present within the rostral half of the PVT (rPVT) compared to the caudal half (cPVT; E, F). LPS treatment produced a small yet significant increase in the number and proportion of

double-labeled (activated) neurons in the rPVT, but not in the cPVT, compared to saline control treatment (see Fig. 5 and Table 1). *4V=fourth ventricle*.

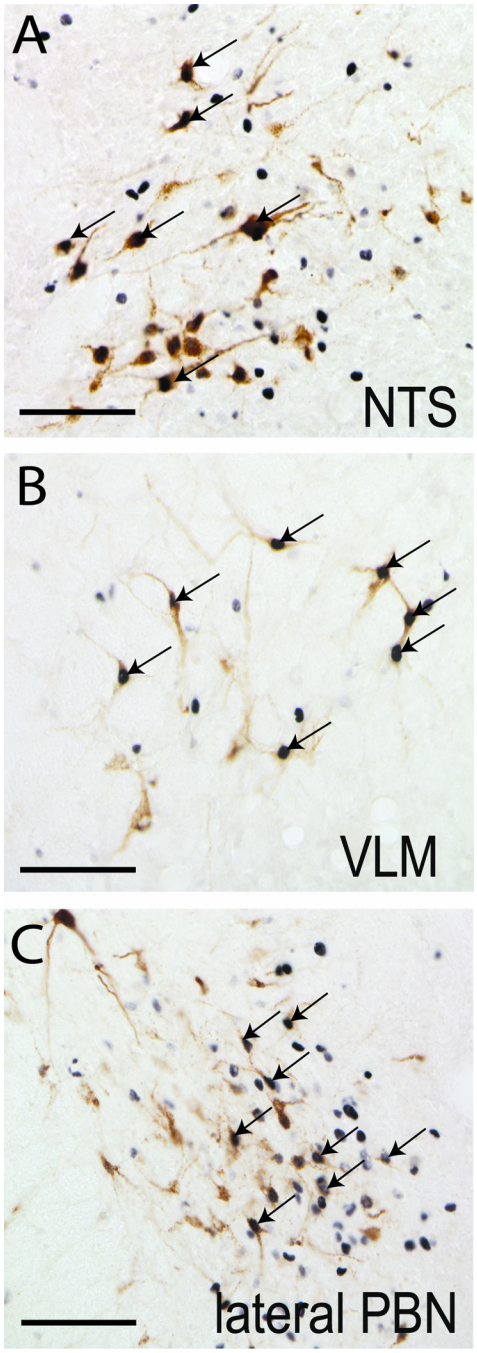

Figure 3. LPS-induced Fos activation of brainstem vlBNST afferents

LPS treatment activated vlBNST-projecting neurons within the NTS (A), VLM (B), and lateral PBN (C), as evidenced by Fos expression (black nuclear staining) within retrogradely-labeled neurons (brown cytoplasmic labeling). Arrows point out examples of double-labeled neurons. Scale bars = 100 μm.

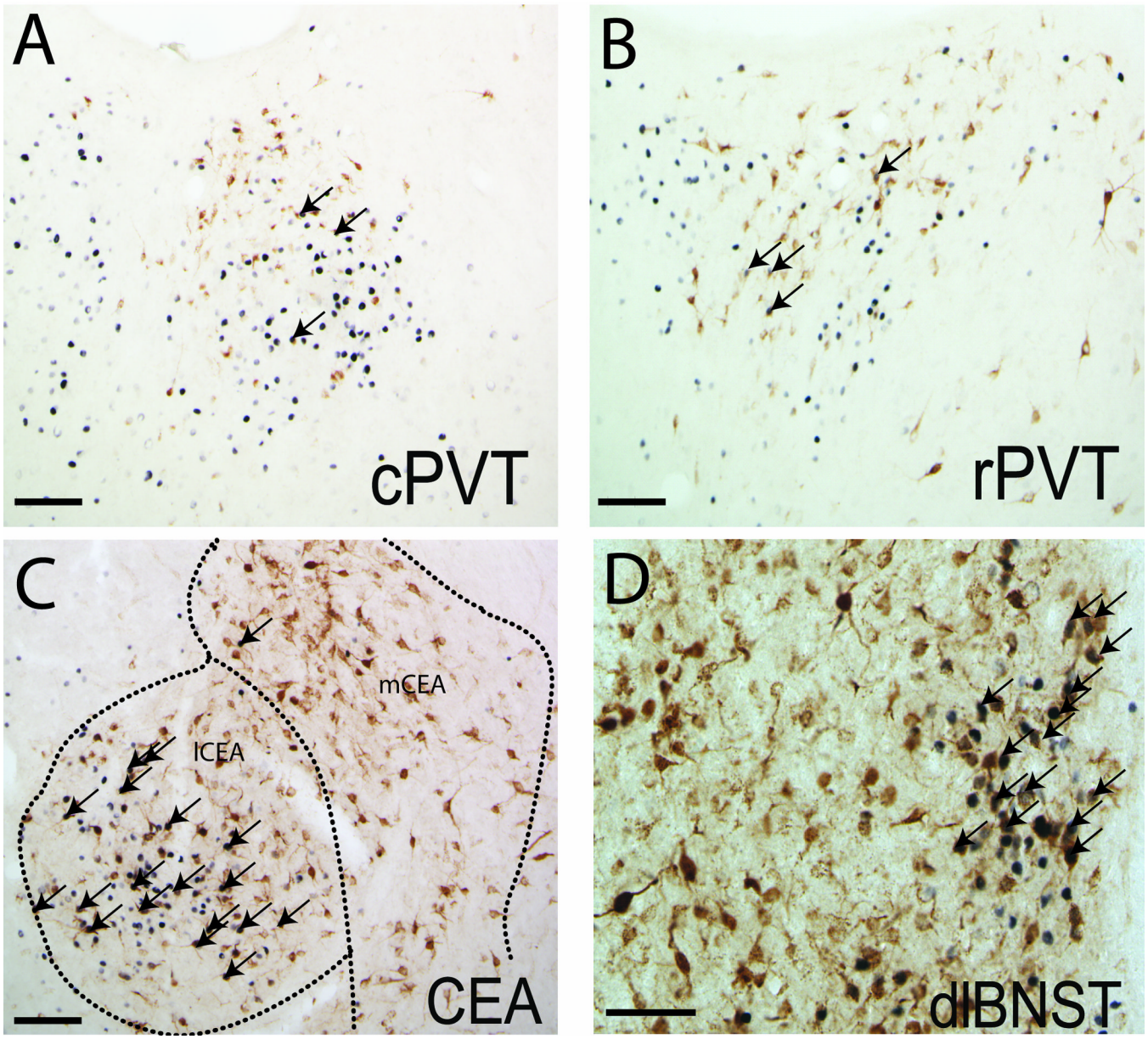

Figure 4. LPS-induced Fos activation of forebrain vlBNST afferents

Despite the presence of numerous retrogradely-labeled neurons and a relatively high incidence of Fos expression within the caudal (A) and rostral PVT (B), relatively few double-labeled neurons were observed in rats after LPS treatment. Conversely, many retrogradely-labeled neurons in the lCEA (C) and dlBNST (D, particularly prevalent within the oval subnucleus) expressed Fos in rats after LPS treatment. Arrows point out examples of double-labeled neurons. Scale bars = 100 μm.

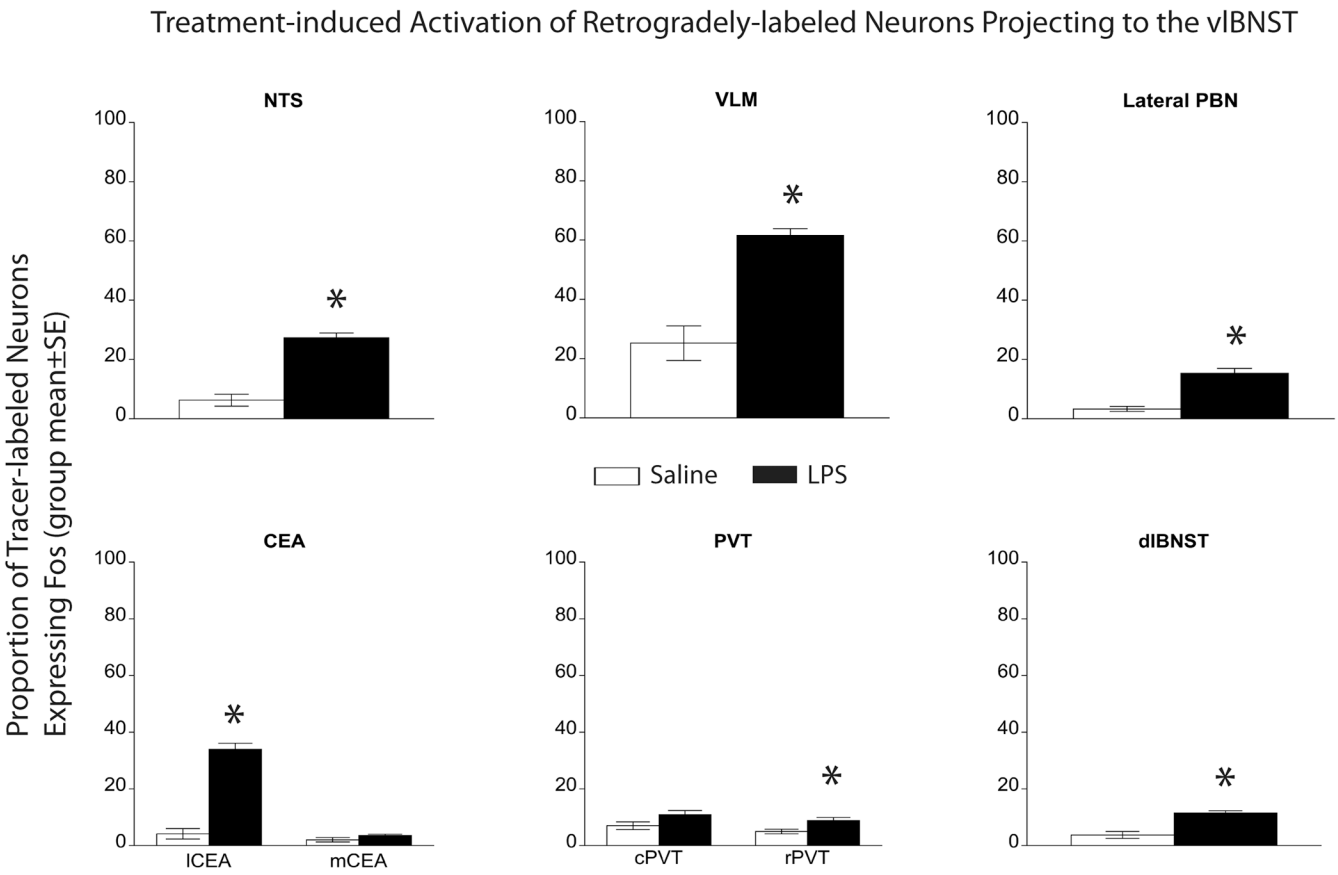

Figure 5. Proportion of activated vlBNST afferents in LPS vs saline rats

The proportion of tracer-labeled neurons that also were Fos-positive (i.e., double-labeled) was significantly increased within the NTS, VLM, lateral PBN, lCEA, and dlBNST in LPS-treated rats (n=8) compared to saline-injected controls (n=6). Small but still significant increases in activation also were observed within the rPVT in LPS-treated rats vs. controls. Conversely, there was no significant effect of LPS treatment on Fos activation of retrogradely labeled neurons within either the mCEA or the cPVT.

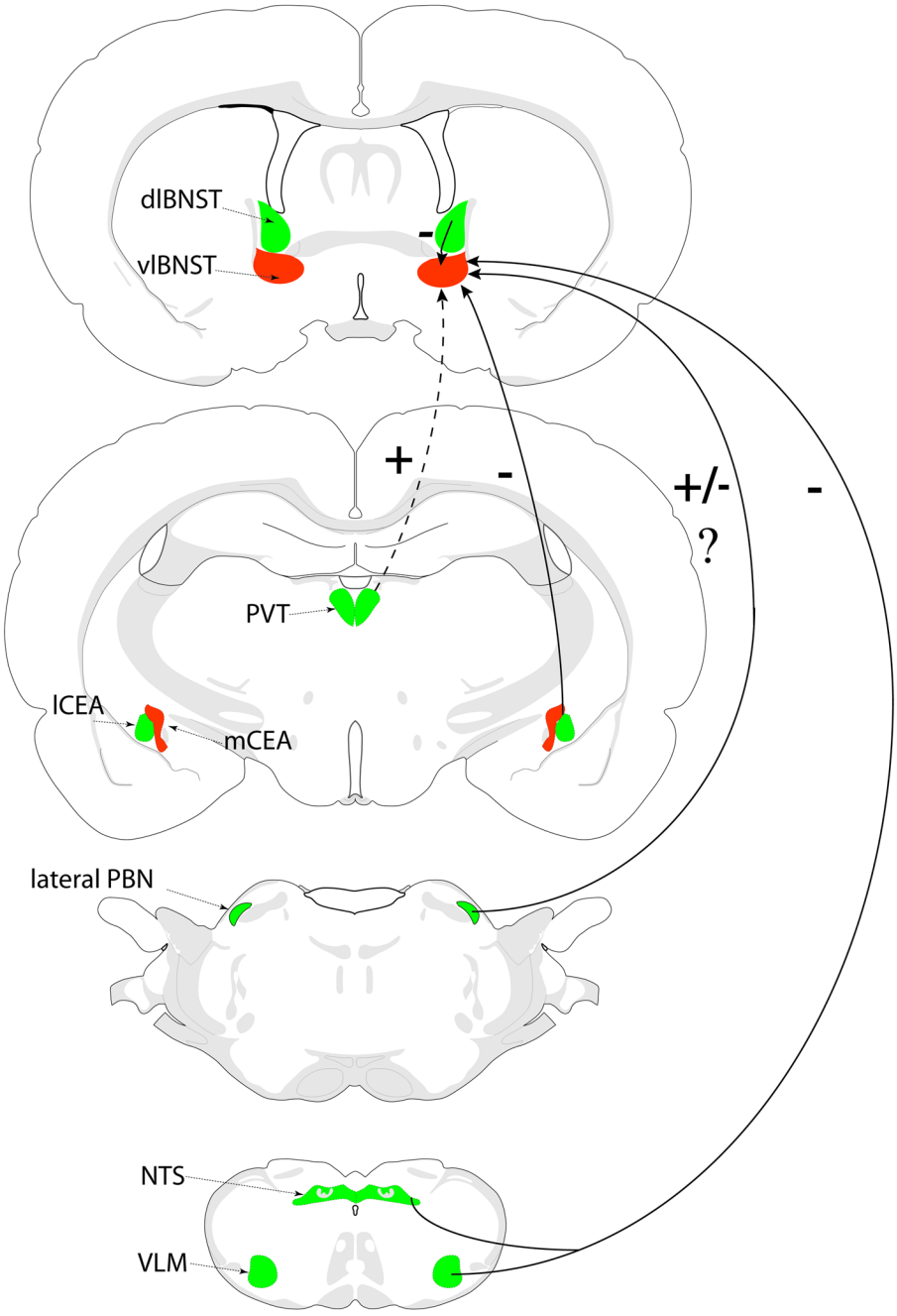

Figure 6. vlBNST inputs converge to promote inhibition of vlBNST activity

Summary diagram of neural inputs to the vlBNST that are recruited/activated (green) or not recruited/activated (red) in response to acute immune challenge with LPS. Together with previous findings, the results of this study suggest that activated neural inputs from the NTS, VLM, lateral PBN, lCEA, and dlBNST converge to promote inhibition of the vlBNST in rats after LPS treatment. Conversely, glutamatergic inputs from the PVT and mPFC (not shown) are weakly activated or not activated in rats after LPS treatment. +, presumably excitatory pathway; −, presumably inhibitory pathway; +/−?, unknown impact. Dashed line, minimal LPS-induced recruitment of this pathway. See text for details.

Table 1

Quantification of double-labeled neurons and proportion of activation in rats after LPS or control saline treatment

Average number of double-labeled neurons and proportion activated to express Fos in rats after systemic LPS (n=8) or saline injection (n=6). LPS significantly increased the number of double-labeled neurons in the NTS, VLM, lateral PBN, lCEA, rPVT and dlBNST. The difference between LPS- and saline-treated rats in the number of double-labeled neurons failed to reach significance in the mCEA and cPVT. Similar to statistical comparisons of the total number of activated neurons, the proportions of retrogradely-labeled neurons that were activated to express Fos in LPS-treated vs. saline-treated rats was significantly increased in the NTS, VLM, lateral PBN, lCEA, rPVT, and dlBNST. For each between-group comparison, ANOVA degrees of freedom = (1,13).

Number and Proportion of Retrogradely-labeled Neurons Activated in Saline control vs. LPS-Treated Rats (group mean±SE)				
Brain Region		**Saline control**	**LPS**	**F statistic and significance**
NTS	# dbl-labeled neurons	11±4	**40±3***	F=42.29 *P*< 0.005
	Proportion activated	6%±2	**27%±2***	F=68.84 *P*< 0.005
VLM	# dbl-labeled neurons	22±8	**49±5***	F=10.08 *P*=0.008
	Proportion activated	25%±6	**62%±2***	F=41.92 *P*< 0.005
lateral PBN	# dbl-labeled neurons	4±1	**16±4***	F=6.33 *P*=0.027
	Proportion activated	3%±1	**15%±2***	F=35.50 *P*< 0.005
lCEA	# dbl-labeled neurons	9±5	**50±10***	F=7.98 *P*=0.015
	Proportion activated	4%±2	**34%±2***	F=103.57 *P*< 0.005
mCEA	# dbl-labeled neurons	6±2	8±2	F=0.31 *P*=0.589
	Proportion activated	2%±1	4%±1	F=2.55 *P*=0.137
cPVT	# dbl-labeled neurons	11±2	20±3	F=3.61 *P*=0.082
	Proportion activated	7%±1	11%±1	F=3.79 *P*=0.075
rPVT	# dbl-labeled neurons	15±3	**28±4***	F=5.38 *P*= 0.039
	Proportion activated	5%±1	**9%±1***	F=8.21 *P*=0.014
dlBNST	# dbl-labeled neurons	13±4	**64±8***	F=29.07 *P*< 0.005
	Proportion activated	2%±1	**11%±1***	F=57.42 *P*< 0.005